International Communications in Heat and Mass Transfer 46 (2013) 126–133

Contents lists available at SciVerse ScienceDirect

International Communications in Heat and Mass Transfer

journal homepage: www.elsevier.com/locate/ichmt

Computational analysis of natural convection in a parallelogrammic cavity with a hot concentric circular cylinder moving at different vertical locations ☆

Ahmed Kadhim Hussein

Mechanical Engineering Department, Babylon University, Babylon City, Iraq

ARTICLE INFO

Available online 4 June 2013

Keywords:
Natural convection
Parallelogrammic cavity
Concentric cylinder
Vertical location

ABSTRACT

A finite volume numerical simulation of natural convection in a parallelogrammic air-filled cavity having a heated concentric circular cylinder is performed. The left and right sidewalls of the cavity are maintained at a uniform cold temperature, while both upper and lower walls of it are considered thermally insulated. A wide range of significant parameters such as Rayleigh number, inclination angle and cylinder vertical locations are considered in the present study. Comparison with previously published works is made and found to be an excellent agreement. The results show that the strength of the flow circulation and the thickness of thermal boundary layer around the hot circular cylinder are increased dramatically when the Rayleigh number increases. Also, to increase the flow circulation inside the parallelogrammic cavity, it is recommended to make the inner cylinder moves downward until it reaches to [$\delta = -0.2$] and the parallelogrammic cavity sidewalls inclined to [$\Phi = 15°$]. Moreover, it is found that for various values of the inclination angle, the average Nusselt numbers at inner cylinder surface and at both cavity sidewalls, decrease when the cylinder moves upward, while they increase when the cylinder moves downward.

1. Introduction

Natural convection in cavities has received much interest in recent years due to its various engineering applications such as energy storage system, furnace engineering, buildings heating and cooling, solar energy collectors and cooling of electronic equipments [1]. In natural convection, a fluid (gas or liquid) circulates between a warm wall and a cold wall due to the density difference. This phenomenon is also called as a force of gravity circulation. Extensive published research works are studied this phenomena either numerically or experimentally under different boundary conditions [2–5]. In addition, natural convection from a circular cylinder embedded in a cavity has many engineering applications such as industrial heat exchanger, cooling system of machine parts and electronic packages. Tasnim et al. [6] investigated numerically the natural convection heat transfer of fluid surrounded an isothermal circular cylinder in a square cavity. They concluded that eccentric positions of the cylinder showed higher heat transfer rate than concentric position. Kumar De and Dalal [7] investigated numerically the natural convection around a square, horizontal, heated cylinder placed in an enclosure. It was found that the overall heat transfer was a function of aspect ratio. Jami et al. [8] performed a numerical investigation of laminar natural convection flows in a differentially heated, square enclosure with a heat-conducting cylinder at its center by using the lattice Boltzmann method. The results were presented for Prandtl number (Pr = 0.71), Rayleigh numbers of ($Ra = 10^3$–10^6) and temperature difference ratio of ($\Delta T = 0$–50). They concluded that independently of the value of (ΔT), the maximum temperature in the cavity decreased with increasing Rayleigh number. Bararnia et al. [9] studied numerically the natural convection around a horizontal elliptic cylinder inside a square enclosure. The results showed that streamlines, isotherms and the number, size and formation of the cells strongly depended on the Rayleigh number and the inner cylinder position. Xu et al. [10] carried out a numerical study of laminar natural convection around a horizontal cylinder inside a concentric air-filled triangular enclosure. The enclosure was filled with air, and both the inner and the outer cylinders were maintained at uniform temperatures. They concluded that the flow intensity and overall heat transfer were significantly enhanced with increasing Rayleigh number due to more contribution from natural convection. Also, as the aspect ratio was enlarged, the overall heat transfer was enhanced, but the flow intensity was diminished. Ghasemi et al. [11] investigated numerically using the control volume finite element method (CVFEM) the natural convection heat transfer in a cold outer circular enclosure containing a hot inner elliptic cylinder. Both of the circular enclosure and the inner cylinder were maintained at constant temperatures with air-filled inside the enclosure. The numerical calculations were performed for various Rayleigh numbers, inclination angle of the enclosure and different sizes of inner cylinder. The results showed that streamlines, isotherms and the number, size and formation of cells inside the enclosure were strongly depended on these parameters, which considerably enhanced the heat transfer rate. Ekundayo et al. [12] investigated numerically the natural convective heat transfer from a horizontal cylinder inserted in a rectangular enclosure. Sidik and Abdul Rahman [13] investigated numerically using the

☆ Communicated by W.J. Minkowycz.

E-mail address: ahmedkadhim74@yahoo.com.

0735-1933/$ – see front matter.
http://dx.doi.org/10.1016/j.icheatmasstransfer.2013.05.008

Nomenclature

Symbol	Description, unit
g	Gravitational acceleration, m/s^2
H	Height of the parallelogrammic cavity, m
Nu	Local Nusselt number
$\overline{\mathrm{Nu}}$	Average Nusselt number
n	Normal direction with respect to the cavity left sidewall
P	Dimensionless pressure
p	Pressure, N/m^2
Pr	Prandtl number
R	Cylinder radius, m
Ra	Rayleigh number
T	Temperature, K
U	Horizontal dimensionless velocity component
u	Horizontal velocity component, m/s
V	Vertical dimensionless velocity component
v	Vertical velocity component, m/s
W	Width of the parallelogrammic cavity, m
X	Dimensionless coordinate in horizontal direction
x	Cartesian coordinate in horizontal direction, m
Y	Dimensionless coordinate in vertical direction
y	Cartesian coordinate in vertical direction, m

Greek Symbols

α	Thermal diffusivity, m^2/s
θ	Dimensionless temperature
Φ	Cavity sidewalls inclination angle, degree
δ	Vertical location of the cylinder
ρ	Density, kg/m^3
ψ	Dimensionless stream function

Subscripts

c	Cold
h	Hot
s	Surface
x	First derivative with respect to x-axis
xx	Second derivative with respect to x-axis
Y	First derivative with respect to Y-axis
YY	Second derivative with respect to Y-axis

lattice Boltzmann scheme, the fluid flow behavior and the heat transfer mechanism from a heated square cylinder located at various heights inside an enclosure in the range of $10^3 \le \mathrm{Ra} \le 10^6$. They concluded that the heat transfer mechanisms were critically dependent on the location of the inner heated square cylinder and the value of Rayliegh numbers. Park et al. [14] investigated numerically using the finite volume method, the natural convection in a square enclosure with hot and cold cylinders, induced by the temperature difference between a cold enclosure and the hot and cold circular cylinders contained within it. The existence of local peaks for Nusselt numbers along surfaces of the cylinders and enclosure was determined by the gap between the cylinders and the enclosure and the thermal plume governed by the convection, respectively. Another useful works can be found in [15–19]. From the other side, real cavities occurring in practice always have geometries different from classical square or rectangular cavities such as parallelogrammic cavities. This complex geometry can be used in many applications such as greenhouses, panels of electronic equipment, sun drying of crops and solar energy collectors. One of the earliest studies on natural convection in parallelogrammic cavities was performed by Yüncü and Yamaç [20], who simulated the laminar natural convection in a parallelogramic air-filled cavity bounded by two isothermal and two insulated walls. Costa [21] studied numerically the double-diffusive natural convection in parallelogrammic enclosures filled with moist air. The heat and mass transfer characteristics of the parallelogrammic enclosure were analyzed using streamlines, heatlines and masslines. He concluded that the global Nusselt and Sherwood numbers were strongly dependent on the thermal Rayleigh number, aspect ratio and inclination angle of the enclosure. Baïri [22] investigated the transient free convection in passive buildings using two-dimensional air-filled parallelogram-shaped enclosures with discrete isothermal heat sources. The temporal evolution of the local and average Nusselt numbers at each band of the hot wall was presented. Saleh et al. [23] investigated numerically the natural convection in a parallelogrammic enclosure filled with nanofluids. The effect of the base angle of the parallelogrammic enclosure on flow and temperature patterns and the heat transfer rate within the enclosure were presented. Very recently, Baïri [24] suggested correlations of the type of Nusselt–Rayleigh–Fourier numbers for transient natural convection in parallelogrammic cavities with isothermal hot wall. The active vertical walls of these cavities were considered vertical, maintained isothermal and differentially heated, while the closing channel was adiabatic. The results were presented for Rayleigh number ($1.84 \times 10^5 \le \mathrm{Ra} \le 1.70 \times 10^9$) and different angles of inclination ranging from ($-60°$ to $60°$). His correlations were obtained from numerical results based on the finite volume method and were validated by measurements. Baïri and Garcia de Maria [25] studied numerically the transient natural convection heat transfer in air-filled convective diode (parallelogrammic) cavities. The results were presented in terms of Nusselt–Rayleigh–Fourier numbers correlations. Their correlations were valid for the specific configuration of the hot wall that consisted of three horizontal, isothermal discrete bands separated by two adiabatic ones of the same dimensions. The channel that connected the hot and cold walls was considered adiabatic and was inclined between $-60°$ and $+60°$ with respect to the horizontal. However, it can be seen from the above literature survey and according to the author's knowledge, that no works up to now were focused on the natural convection from a concentric circular cylinder inserted in a parallelogrammic cavity. Therefore, this is the first paper which considered this problem in detail.

2. Mathematical formulation

2.1. Geometrical configuration and governing equations

A concentric heated circular cylinder of radius (R) located inside an air-filled parallelogrammic cavity of height (H) and width (W) where [$H = W$] is shown in Fig. 1. Natural convection phenomena occurs between the cylinder surface, which is maintained at a uniform hot temperature (T_h), and the cavity left and right sidewalls, which are maintained at a uniform cold temperature (T_c). The upper and the lower walls of the cavity are considered thermally insulated. The flow field and heat transfer are assumed to be two-dimensional laminar and steady. No-slip boundary conditions are assumed at solid boundaries (i.e., $U = V = 0$). The Boussinesq approximation is invoked to relate density changes to temperature changes while the other properties of the fluid are considered constant. The study parameters are Rayleigh number (Ra) varying from 10^3 to 10^7 inclination angle (Φ) varying as (0°,15° and 30°), while the cylinder radius and the Prandtl number are considered constant at ($R = 0.2$) and ($\mathrm{Pr} = 0.71$), respectively. The cylinder moves upward and downward along the vertical centerline of the cavity at different vertical locations varying as [$\delta = 0, \pm 0.1$ and ± 0.2]. The dimensionless governing equations (continuity, momentum and energy equations) for the present work can be written in the following form:

$$U_X + V_Y = 0 \tag{1}$$

$$UU_X + VU_Y = -P_X + Pr(U_{XX} + U_{YY}) \tag{2}$$

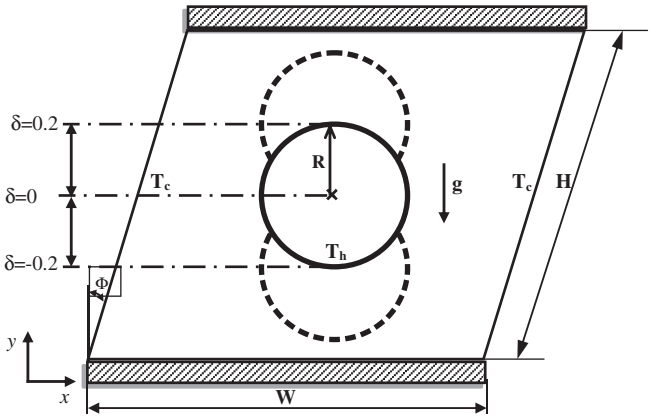

Fig. 1. Schematical configuration of considered model with boundary conditions.

$$UV_X + VV_Y = -P_Y + \Pr[V_{XX} + V_{YY}] + Ra \Pr \theta \tag{3}$$

$$U\theta_X + V\theta_Y = (\theta_{XX} + \theta_{YY}) \tag{4}$$

Eqs. (1–4) are obtained by using the following dimensionless parameters as follows:

$$X = \frac{x}{W}, Y = \frac{y}{W}, U = \frac{uW}{\alpha}, V = \frac{vW}{\alpha},$$

$$P = \frac{pW^2}{\rho\alpha^2}, \theta = \frac{T - T_c}{T_h - T_c} \tag{5}$$

The dimensionless boundary conditions are given as follows:

1 The upper and the lower walls of the parallelogrammic cavity are considered thermally insulated, i.e.,

at $Y = 0$ and $Y = 1$ $\theta_Y = 0$

2 The left and the right sidewalls of the parallelogrammic cavity are maintained at uniform cold temperature (T_c), i.e.,

$$0 \le X \le \sin(\Phi) \text{ and } 1 \le X \le 1 + \sin(\Phi), \theta = 0$$

The average Nusselt number ($\overline{Nu}$) is represented as follows:

$$\overline{Nu} = \frac{1}{H}\int_0^H \left[\frac{\partial\theta}{\partial n}\right]_s \mathrm{dn} \tag{6}$$

3. Computational details, grid independence test and results validation

The mass, momentum and energy equations (Eqs. (1)–(4)) are a mixture set of elliptic-parabolic partial differential equations, which are solved by using the finite volume method with a collocated grid system. The finite volume method is a powerful tool for solving partial differential equations. The Tri-Diagonal Matrix Algorithm (TDMA) solver is used in the computation process. For full details about the solution technique by using this method, see Hoffmann [26]. To check the iterative solution convergence, the summation of the absolute differences of the solution variables between two successive iterations has been calculated. When this summation becomes below the convergence criterion which is selected as 10^{-7}, the iteration process will be terminated. Fine grids are used in regions with steep temperature and velocity gradients. To get a grid test for the present work, a grid independent solution is performed. The results are represented in terms of average Nusselt number along the hot inner circular cylinder surface with grid refinement as shown in Fig. 2. The test is carried out at Ra $=10^7$, $\delta = -0.2$ and $\Phi = 15°$ and 30°. The results show that a number of (10,000) control volumes satisfies the requirements of the grid independence study where no significant variation can be found in the average Nusselt number for both $\Phi = 15°$ and 30°. In order to validate the numerical results of the present work both problems of natural convection in a square enclosure with a circular cylinder inside it (Kim et al. [27]) and the natural convection in the annulus between concentric horizontal circular and square cylinders (Moukalled and Acharya [28]) are solved numerically using the developed computer program of the present work. The computed results are compared with the results of Kim et al. [27] and Moukalled and Acharya [28], as shown in Table 1. Good agreements are seen between the results computed by the present computer program with those of Kim et al. [27] and Moukalled and Acharya [28], respectively.

4. Results and discussion

4.1. Flow and thermal fields

The effects of the Rayleigh number (Ra), cavity sidewalls inclination angle (Φ) and vertical locations of circular cylinder (δ) on the flow and thermal fields by using streamlines (on the left) and isotherms (on the right) are shown in Figs. 3 and 4. When the Rayleigh number is low (Ra $= 10^4$), the circulation vortices are weak as shown in Fig. 3. In this case, the effect of the natural convection is slight. In general, the flow field inside the parallelogrammic cavity is characterized by a two major rotating vortices around the inner circular cylinder. The natural convection currents are generated due to the temperature difference between the hot circular cylinder and the cold sidewalls of the parallelogrammic cavity. The isotherms are generally undistorted, and they are like horizontal lines and in this case the heat conduction is dominant. Moreover, the thermal boundary layer thickness around the hot circular cylinder is very slight for different values of inclination angle and vertical locations of circular cylinder. The maximum stream function when the Rayleigh number is low (Ra $= 10^4$) can be seen at [$\Phi = 0°$ and $\delta = -0.2$], which is [$\psi = 2.07524$]. As the

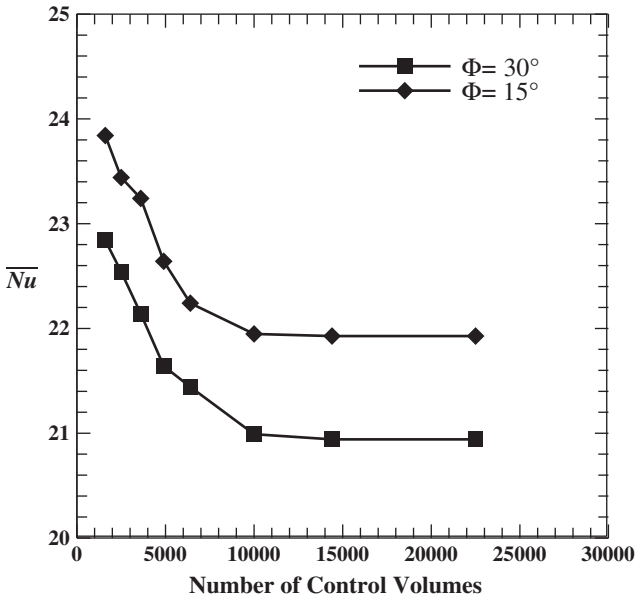

Fig. 2. Grid independent test of average Nusselt number along the hot inner circular cylinder surface with grid refinement at Ra $= 10^7$, $\delta = -0.2$, $\Phi = 15°$ and 30°.

Table 1
Comparison of present surface-average Nusselt number with those of previous numerical studies.

Ra	Average Nusselt Number at the hot wall			Error (%)
	Present study	Kim et al. [27]	Moukalled and Acharya [28]	
10^3	3.4047	3.414	3.331	−2.2125
10^4	5.12893	5.1385	5.08	−1.96318
10^5	9.38875	9.3900	9.374	−0.1573
10^6	15.6995	15.665	15.79	0.57314

Rayleigh number jumps to ($Ra = 10^7$), both streamlines and isotherms are convert completely from uniform shape to non-uniform one as shown in Fig. 4. This conversion indicating a remarkable strong circulation occurs in this case and the natural convection effect becomes very strong. Thus, isotherms are clustered adjacent the hot circular cylinder inside the cavity. Also, the thickness of the thermal boundary layer increases significantly especially around the circular cylinder. The maximum stream function when the Rayleigh number is high ($Ra = 10^7$) can be seen at [$\Phi = 15°$ and $\delta = -0.2$], which is [$\psi = 38.027$]. Therefore, from the above discussion, it can be concluded that the Rayleigh number plays a remarkable role to control the shape of both the circulation vortices and the isotherms. Also, it is a control key to indicate the mechanism of the heat transfer inside the parallelogrammic cavity. With respect to the effect of the cavity sidewalls inclination angle (Φ) and vertical locations of circular cylinder (δ) on the flow and thermal fields inside the parallelogrammic cavity, it can be observed that when the inclination angle (Φ) is zero [i.e., square cavity case], the flow field are approximately symmetrical around the circular cylinder. But as the inclination angle increases to [$\Phi = 15°$] and [$\Phi = 30°$], respectively, various shapes of vortices can be observed depending on the vertical locations of circular cylinder (δ). When [$Ra = 10^4$] and [$\delta = 0$], or in other words the cylinder located at the center of the parallelogrammic cavity, the strength of the flow circulation increases from [$\psi = 1.14408$] to [$\psi = 1.19088$] as the inclination angle increases, respectively, from [$\Phi = 0°$] to [$\Phi = 30°$] as shown in Fig. 3. In this case, the two major vortices around the cylinder begin to enlarge along the diagonal of the parallelogrammic cavity as the inclination angle increases. While at [$Ra = 10^7$] and [$\delta = 0$], the strength of the flow circulation decreases from [$\psi = 27.275$] to [$\psi = 25.9024$] as the inclination angle increases, respectively, from [$\Phi = 0°$] to [$\Phi = 30°$] as shown in Fig. 4. In this case, the uniform shape of vortices around the cylinder destroys due to the strong effect of convection. Now, when [$Ra = 10^4$] and the cylinder moves vertically upward [i.e., when $\delta = +0.1$ and $\delta = +0.2$], the vortices size begin to increase in the region below the inner cylinder. This is because the space between the cylinder surface and the upper horizontal

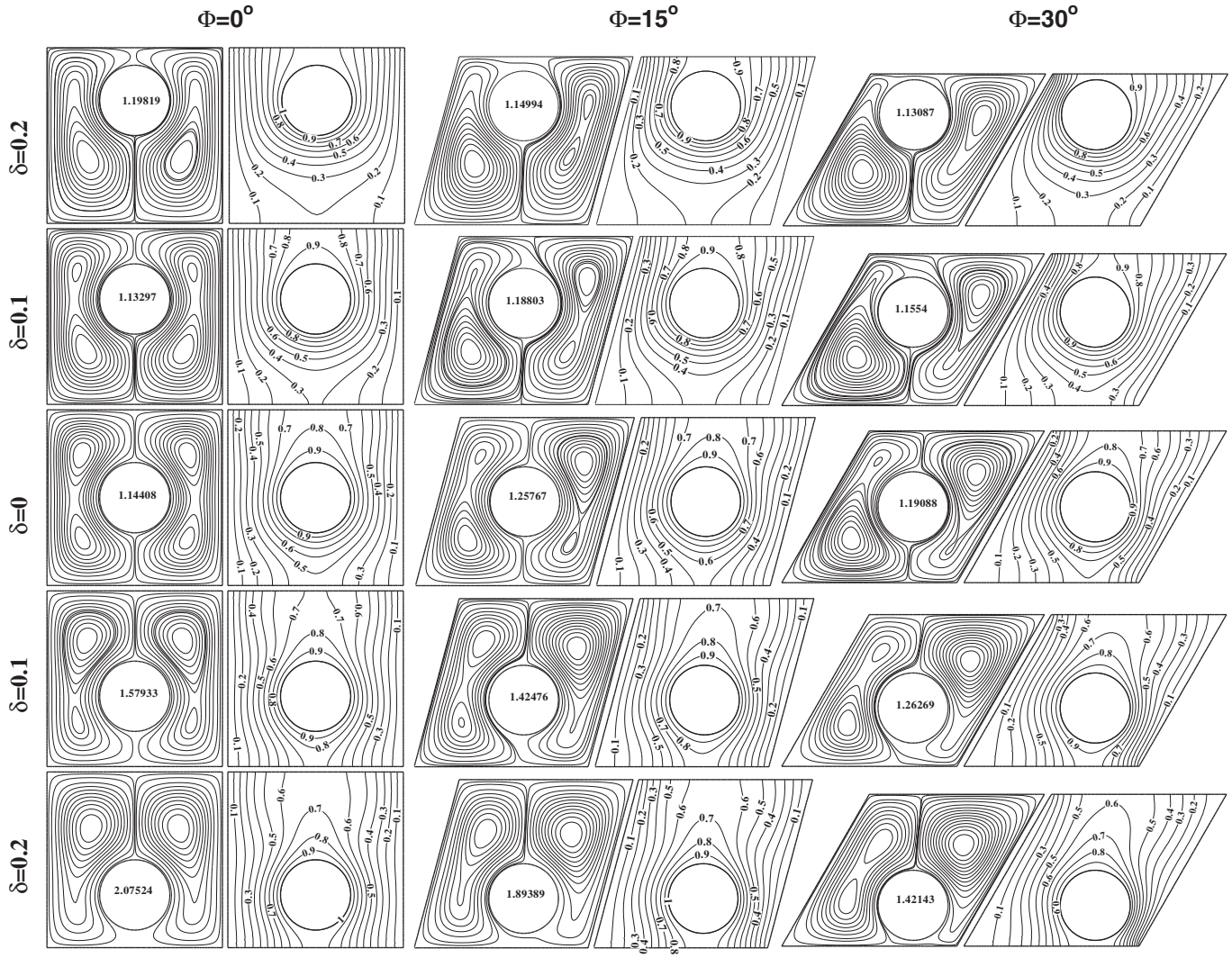

Fig. 3. Distribution of streamlines (on the left) within values of $|\psi|_{max}$ and isotherms (on the right) for different vertical locations of circular cylinder (δ) and sidewall inclination angles (Φ) at $Ra = 10^4$.

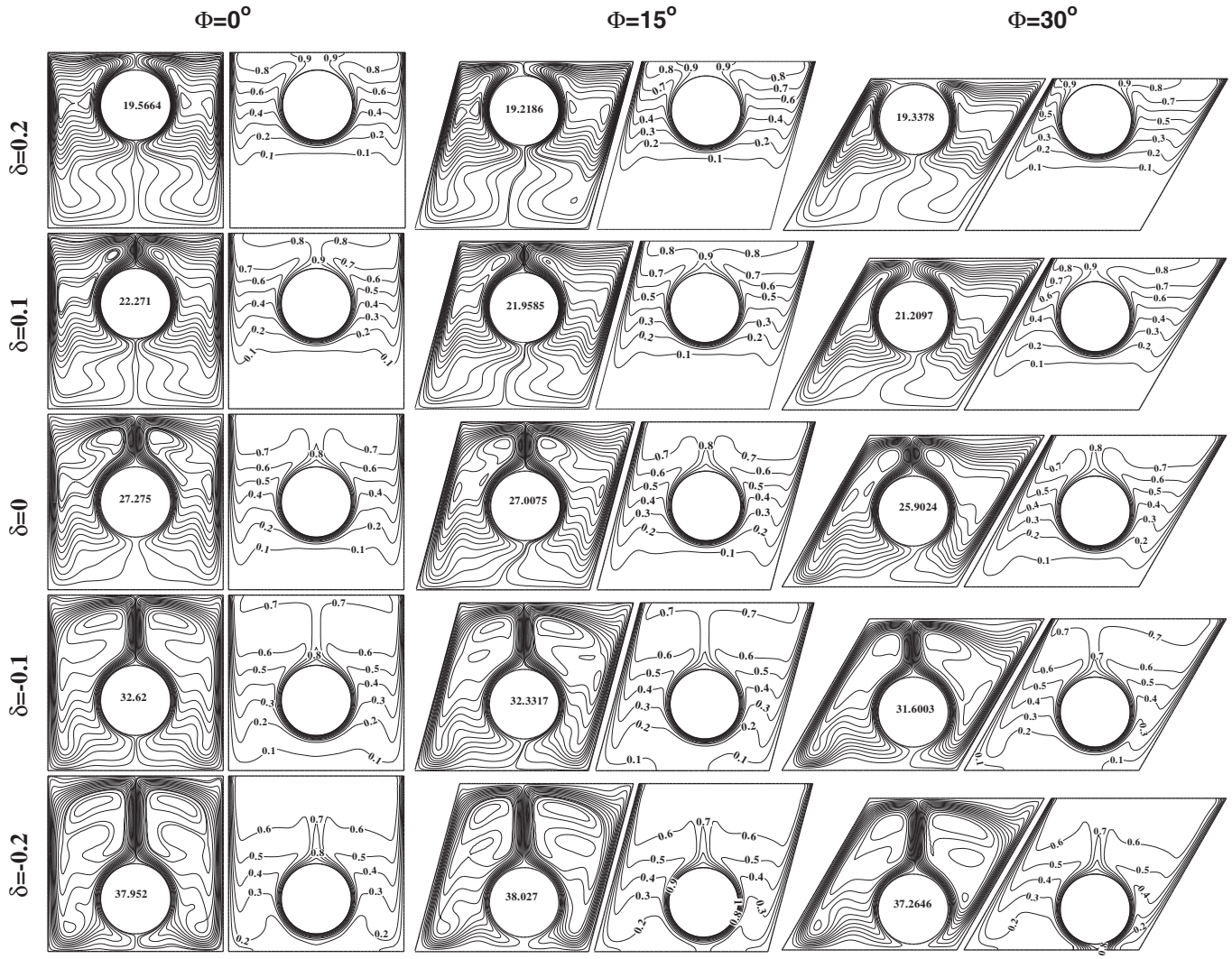

Fig. 4. Distribution of streamlines (on the left) within values of $|\psi|_{max}$ and isotherms (on the right) for different vertical locations of circular cylinder (δ) and sidewall inclination angles (Φ) at Ra $= 10^7$

wall decreases as the cylinder moves vertically upward leading to push the vortices to extend below the inner cylinder. When [$\Phi = 0°$] and as the vertical locations of circular cylinder (δ) increases from [$\delta = +0.1$] to [$\delta = +0.2$], the strength of the flow circulation increases from [$\psi = 1.13297$] to [$\psi = 1.19819$]. A reverse behavior can be noticed when the inclination angle increases to [$\Phi = 15°$] and [$\Phi = 30°$]. The maximum strength of the flow circulation can be found at [$\Phi = 0°$] and [$\delta = +0.2$], which is [$\psi = 1.19819$], while the minimum strength of the flow circulation can be found at [$\Phi = 30°$] and [$\delta = +0.2$], which is [$\psi = 1.13087$]. At [Ra $= 10^7$], the strength of the flow circulation decreases for all inclination angles [i.e., at $\Phi = 0°$, 15° and 30°] when the cylinder moves vertically upward from [$\delta = +0.1$] to [$\delta = +0.2$]. In this case, the maximum strength of the flow circulation can be found at [$\Phi = 0°$] and [$\delta = +0.1$], which is [$\psi = 22.271$], while the minimum strength of the flow circulation can be found at [$\Phi = 15°$] and [$\delta = +0.2$], which is [$\psi = 19.2186$]. Furthermore, a symmetrical shape of vortices can be seen when [$\Phi = 0°$], while as the inclination angle increases to [$\Phi = 15°$] and [$\Phi = 30°$], the symmetry property between the two vortices are diminished gradually. From the other side, when the cylinder moves vertically downward [i.e., when $\delta = -0.1$ and $\delta = -0.2$], the vortices size begin to increase in the region up the inner cylinder. This is because the region between the cylinder surface and the lower horizontal wall decreases as the cylinder moves vertically downward leading to push the vortices to extend up the inner cylinder. Also, it can be noticed that when the inclination angle increases to [$\Phi = 15°$] and [$\Phi = 30°$], the two vortices inside the parallelogrammic cavity convert from symmetrical pattern, which is found at [$\Phi = 0°$] to unsymmetrical one. When [Ra $= 10^4$] and the cylinder moves vertically downward [i.e., when $\delta = -0.1$ and $\delta = -0.2$], it can be seen that the strength of the flow circulation at [$\Phi = 0°$] increases from [$\psi = 1.57933$] to [$\psi = 2.07524$] when the vertical locations of circular cylinder (δ) decreases from [$\delta = -0.1$] to [$\delta = -0.2$], respectively. The same observation can be found at [$\Phi = 15°$] and [$\Phi = 30°$]. The maximum strength of the flow circulation can be found at [$\Phi = 0°$] and [$\delta = -0.2$], which is [$\psi = 2.07524$], while the minimum strength of the flow circulation can be found at [$\Phi = 30°$] and [$\delta = -0.1$], which is [$\psi = 1.26269$]. At [Ra $= 10^7$], the strength of the flow circulation increases for all inclination angles [i.e., at $\Phi = 0°$, 15° and 30°] when the cylinder moves vertically downward from [$\delta = -0.1$] to [$\delta = -0.2$]. In this case, the maximum strength of the flow circulation can be found at [$\Phi = 15°$] and [$\delta = -0.2$], which is [$\psi = 38.027$], while the minimum strength of the flow circulation can be found at [$\Phi = 30°$] and [$\delta = -0.1$], which is [$\psi = 31.6003$]. With respect to isotherms, it can be noticed from the results of Figs. 3 and 4 that the effect of the cavity sidewalls inclination angle (Φ) and vertical locations of circular cylinder

(δ) on the flow and thermal fields are slight and less than the effect of the Rayleigh number.

4.2. Local Nusselt number results

Fig. 5 demonstrates the variation of the local Nusselt number along the semicircle cylinder surface at different vertical locations of circular cylinder and Rayleigh number for ($\Phi = 0°$) first row, ($\Phi = 15°$) second row and ($\Phi = 30°$) third row, respectively. When the inclination angle (Φ) is zero [i.e., square cavity case] and ($Ra = 10^3$ and $Ra = 10^4$), the local Nusselt number increases for various values of (δ) until the mid-semicircle arc length and then begins to decrease gradually. Generally, it can be seen that when the cylinder moves vertically downward, the local Nusselt numbers are greater than the corresponding values when the cylinder moves vertically upward. This is because the flow circulation increases when the cylinder moves vertically downward as explained above. At [$Ra = 10^5$,10^6 and 10^7], the local Nusselt numbers increase gradually for various values of (δ) until the Rayleigh number reaches to [$Ra = 10^7$]. The exception case from this behavior is only when [$\delta = +0.1$], where a reverse behavior can be observed. This is due to the sudden drop in the temperature gradient at the semicircle cylinder surface which leads to decrease the local Nusselt number. Moreover, the local Nusselt numbers increase as Rayleigh number increases. When the inclination angle increases to [$\Phi = 15°$] and [$\Phi = 30°$], respectively, the local Nusselt numbers increase as the cylinder moves vertically downward and then begin to decrease as the semicircle arc length increases. The decreasing in the local Nusselt number curves becomes slight as the Rayleigh number increases. Also, it can be concluded from Fig. 5, that the local Nusselt numbers increase, as the inclination angle increases especially when the Rayleigh number is low [i.e., $Ra = 10^3$ and $Ra = 10^4$].

4.3. Average Nusselt number results

The variation of average Nusselt numbers at inner cylinder surface [case (a)], cavity right sidewall [case (b)] and cavity left sidewall [case (c)] is shown in Fig. 6 for various values of Rayleigh number (Ra), cavity sidewalls inclination angle (Φ) and vertical locations of circular cylinder (δ). As can be seen from the figure, average Nusselt numbers are increased with the Rayleigh number because the flow circulation is increased when the Rayleigh number increases. This conclusion is found for various values of inclination angle (Φ) and vertical locations of circular cylinder (δ). Also, it can be observed that the average Nusselt numbers at the inner cylinder surface are greater than the corresponding values at the cavity left and right sidewalls. This is an expected result, since the temperature gradient at the hot surface of the cylinder is more than the temperature gradient at the cavity left and right sidewalls. This result is noticed for all values of the inclination angle (Φ). With respect to the effect of vertical locations of circular cylinder (δ) on the average Nusselt numbers, it is seen from Fig. 6 that when [$\Phi = 0°$], the average Nusselt numbers at inner cylinder surface and at both cavity sidewalls decrease when the cylinder moves upward from [$\delta = +0.1$] to [$\delta = +0.2$], while it increases when the cylinder moves downward from [$\delta = -0.1$] to [$\delta = -0.2$]. This is because the strength of the flow circulation at [$\Phi = 0°$] decreases when the cylinder moves upward from [$\delta = +0.1$] to [$\delta = +0.2$]. In contrast, it increases when the cylinder moves downward from [$\delta = -0.1$] to [$\delta = -0.2$]. The same phenomena can be observed when the inclination angle increases to [$\Phi = 15°$] and [$\Phi = 30°$], respectively. Moreover, it is found from Fig. 6 that the average Nusselt numbers grow very slowly when the Rayleigh number is low [i.e., $Ra = 10^3$ and $Ra = 10^4$], giving values similar to the case of conduction. In contrast to the previous situation, the average Nusselt numbers increase markedly when the Rayleigh number is high (i.e., $Ra = 10^7$).

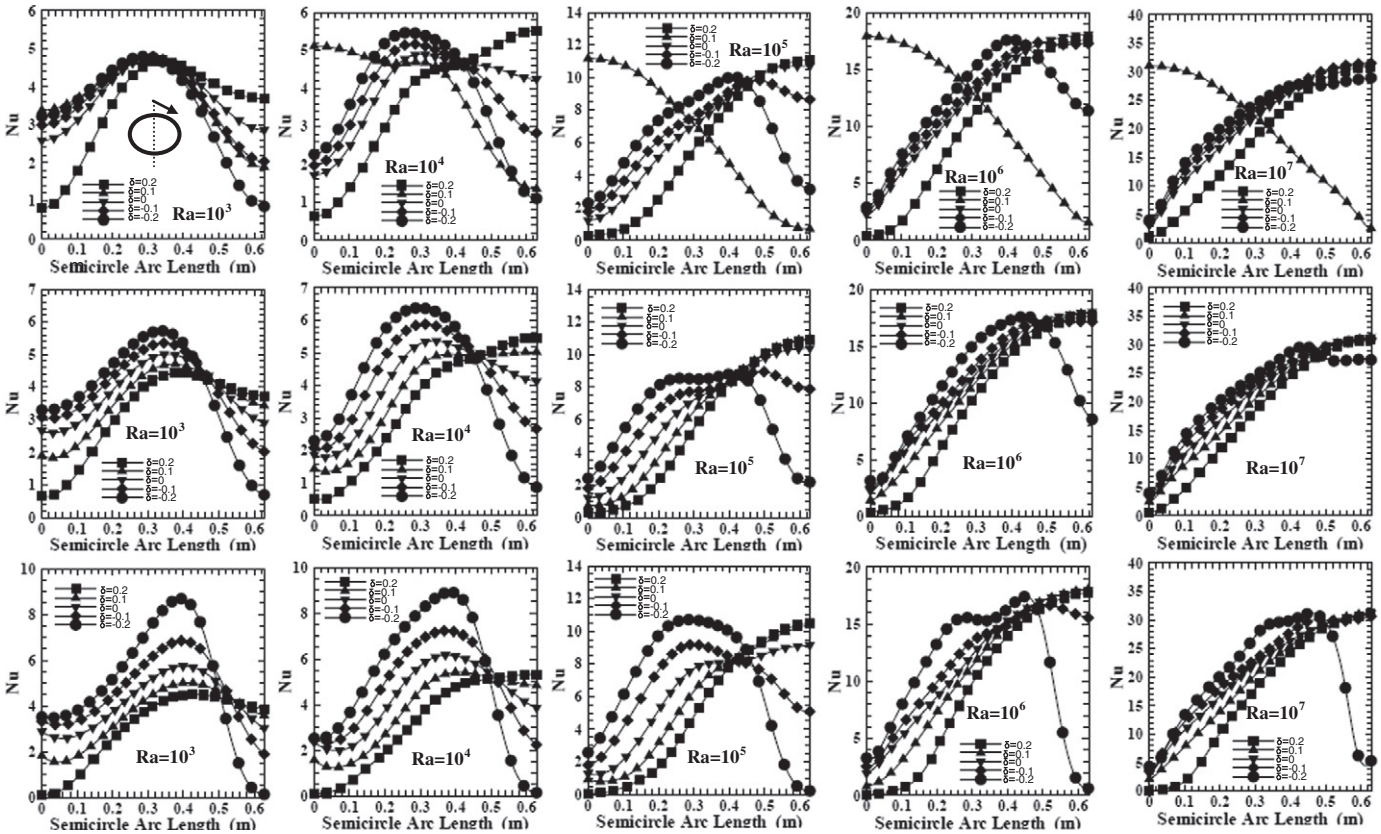

Fig. 5. Variation of local Nusselt number along the inner semicircle cylinder surface at different vertical locations of circular cylinder and Rayleigh number for ($\Phi = 0°$) first row, ($\Phi = 15°$) second row and ($\Phi = 30°$) third row.

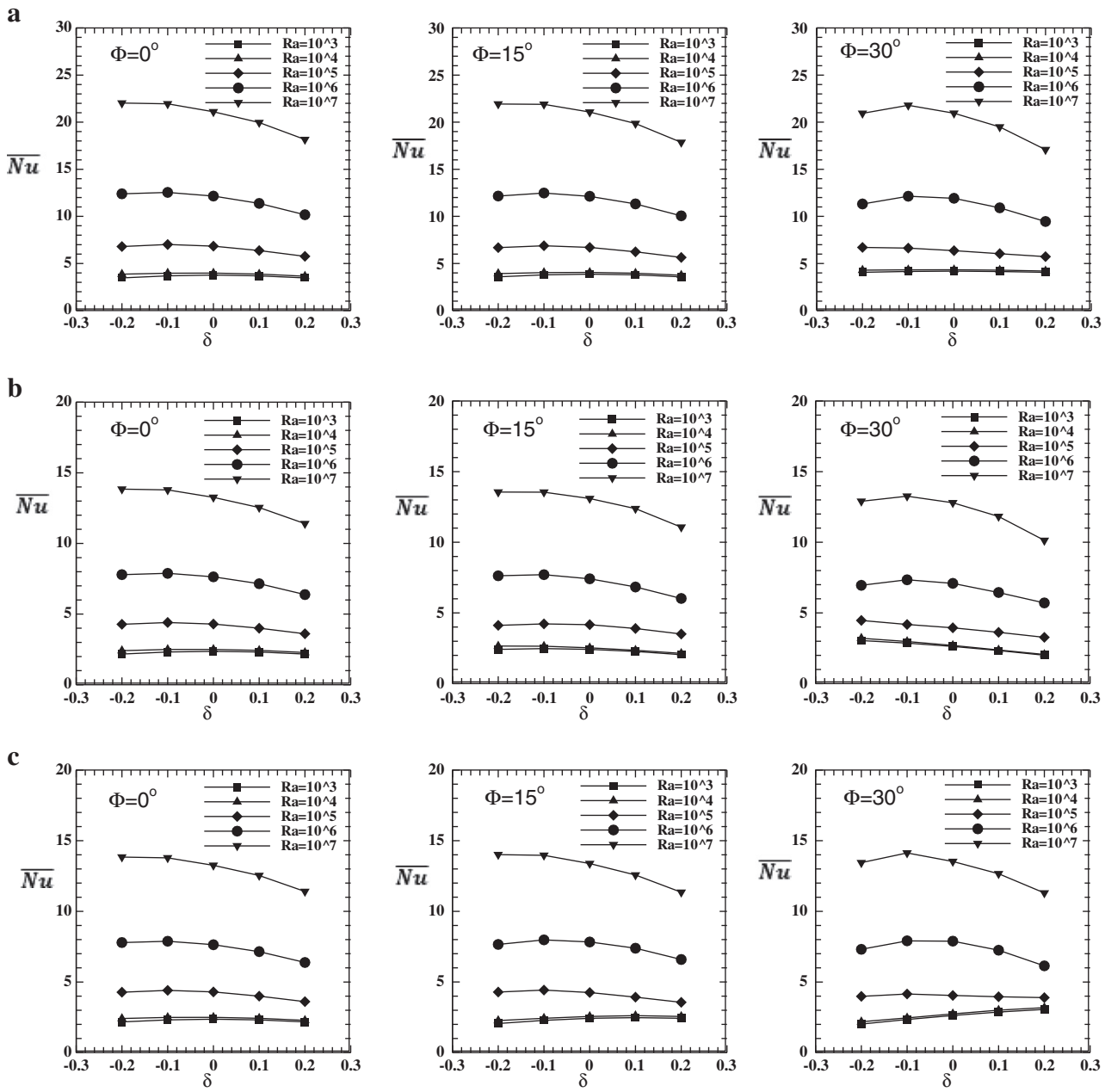

Fig. 6. Variation of surface-averaged Nusselt number as function of δ for the various Rayleigh numbers and side wall inclination angles (Φ) at (a) inner cylinder surface (b) right wall (c) left wall.

This behavior is due to the increase in the temperature gradient as the Rayleigh number increases.

5. Conclusions

The following conclusions can be drawn from the results of the present work:

1 The strength of the flow circulation and the thickness of thermal boundary layer around the hot circular cylinder increase dramatically when the Rayleigh number increases.
2 The heat transfer mechanism is converted from conduction to convection when the Rayleigh number increases.
3 The isotherms are undistorted and like a horizontal lines when the Rayleigh number is low [Ra $= 10^4$]. But at [Ra $= 10^7$], they become completely non-uniform and their shape changes from horizontal lines to semi-curved one.
4 The flow field are approximately symmetrical around the circular cylinder when [$\Phi = 0°$]. But when [$\Phi = 15°$] and [$\Phi = 30°$] various shapes of vortices are seen depending on the vertical locations of circular cylinder (δ).
5 To increase the flow circulation inside the parallelogrammic cavity, it is recommended to make the inner cylinder moves downward until it reaches to [$\delta = -0.2$] and the parallelogrammic cavity sidewalls inclined to [$\Phi = 15°$].
6 When [Ra $= 10^4$] and [$\delta = 0$], the strength of the flow circulation increases as the inclination angle increases to [$\Phi = 30°$]. While at [Ra $= 10^7$] and [$\delta = 0$] the strength of the flow circulation decreases as the inclination angle increases to [$\Phi = 30°$].
7 At [Ra $= 10^4$] and the cylinder moves vertically upward [i.e., when $\delta = +0.1$ and $\delta = +0.2$], the flow circulation strength increases

at [$\Phi = 0°$], while it decreases when the inclination angle increases to [$\Phi = 15°$] and [$\Phi = 30°$]. The maximum flow circulation strength is found at [$\Phi = 0°$] and [$\delta = +0.2$]. At [$Ra = 10^7$], the flow circulation strength decreases for all inclination angles. The maximum flow circulation strength is found at [$\Phi = 0°$] and [$\delta = +0.1$].

8 At [$Ra = 10^4$] and the cylinder moves vertically downward [i.e., when $\delta = -0.1$ and $\delta = -0.2$], the flow circulation strength increases at [$\Phi = 0°$, 15° and 30°]. The maximum flow circulation strength is found at [$\Phi = 0°$] and [$\delta = -0.2$]. The same increasing are found at [$Ra = 10^7$] where the maximum flow circulation strength is found at [$\Phi = 15°$] and [$\delta = -0.2$].

9 The local Nusselt numbers increase as the Rayleigh number increases.

10 The local Nusselt numbers when the cylinder moves vertically downward are greater than the corresponding values when the cylinder moves vertically upward.

11 When the inclination angle increases, the local Nusselt numbers increase, especially when the Rayleigh number is low [i.e., $Ra = 10^3$ and $Ra = 10^4$].

12 It is found that for various values of inclination angle (Φ) and vertical locations of circular cylinder (δ), the average Nusselt numbers are increased continuously when the Rayleigh number increases.

13 For different values of the inclination angle (Φ), the average Nusselt numbers at the inner cylinder surface are more than the corresponding values at the cavity left and right sidewalls.

14 For various values of the inclination angle (Φ), the average Nusselt numbers at inner cylinder surface and at both cavity sidewalls, decrease when the cylinder moves upward while it increases when the cylinder moves downward.

References

[1] D. Moore, D. Newport, V. Egan, V. Lacarac, Ventilation and internal structure effects on naturally induced flows in a static aircraft wing, Applied Thermal Engineering 32 (2012) 49–58.

[2] H. Turkoglu, N. Yucel, Effects of heater and cooler location on natural convection in square cavities, Numerical Heat Transfer 27 (1995) 351–358.

[3] M. Moghimi, H. Mirgolbabaei, Me. Miansari, Mo. Miansari, Natural convection in rectangular enclosures heated from below and cooled from above, Australian Journal of Basic and Applied Sciences 3 (4) (2009) 4618–4623.

[4] O. Turan, N. Chakraborty, R. Poole, Laminar natural convection of Bingham fluids in a square enclosure with differentially heated side walls, Journal of Non-Newtonian Fluid Mechanics 165 (2010) 901–913.

[5] A. Horibe, R. Shimoyama, N. Haruki, A. Sanada, Experimental study of flow and heat transfer characteristics of natural convection in an enclosure with horizontal parallel heated plates, International Journal of Heat and Mass Transfer 55 (2012) 7072–7078.

[6] S. Tasnim, S. Mahmud, P. Das, Effect of aspect ratio and eccentricity on heat transfer from a cylinder in a cavity, International Journal of Numerical Methods for Heat and Fluid Flow 12 (7) (2002) 855–869.

[7] A. Kumar De, A. Dalal, A numerical study of natural convection around a square, horizontal, heated cylinder placed in an enclosure, International Journal of Heat and Mass Transfer 49 (2006) 4608–4623.

[8] M. Jami, A. Mezrhab, M. Bouzidi, P. Lallemand, Lattice Boltzmann method applied to the laminar natural convection in an enclosure with a heat-generating cylinder conducting body, International Journal of Thermal Sciences 46 (2007) 38–47.

[9] H. Bararnia, S. Soleimani, D. Ganji, Lattice Boltzmann simulation of natural convection around a horizontal elliptic cylinder inside a square enclosure, International Communications in Heat and Mass Transfer 38 (2011) 1436–1442.

[10] X. Xu, Z. Yu, Y. Hu, L. Fan, K. Cen, A numerical study of laminar natural convective heat transfer around a horizontal cylinder inside a concentric air-filled triangular enclosure, International Journal of Heat and Mass Transfer 53 (2010) 345–355.

[11] E. Ghasemi, S. Soleimani, H. Bararnia, Natural convection between a circular enclosure and an elliptic cylinder using control volume based finite element method, International Communications in Heat and Mass Transfer 39 (2012) 1035–1044.

[12] C. Ekundayo, S. Probert, M. Newborough, Heat transfer from a horizontal cylinder in a rectangular enclosure, Applied Energy 61 (1998) 57–78.

[13] N. Sidik, M. Abdul Rahman, Mesoscale investigation of natural convection heat transfer from a heated cylinder inside square enclosure, European Journal of Scientific Research 38 (1) (2009) 45–56.

[14] Y. Park, H. Yoon, M. Ha, Natural convection in square enclosure with hot and cold cylinders at different vertical locations, International Journal of Heat and Mass Transfer 55 (2012) 7911–7925.

[15] J. House, C. Beckermann, T. Smith, Effect of a centered conducting body on natural convection heat transfer in an enclosure, Numerical Heat Transfer, Part A 18 (1990) 213–225.

[16] G. Cesini, M. Paroncini, G. Cortellab, M. Manzan, Natural convection from a horizontal cylinder in a rectangular cavity, International Journal of Heat and Mass Transfer 42 (1999) 1801–1811.

[17] B. Kim, D. Lee, M. Ha, H. Yoon, A numerical study of natural convection in a square enclosure with a circular cylinder at different vertical locations, International Journal of Heat and Mass Transfer 51 (2008) 1888–1906.

[18] S. Hussain, A. Hussein, Natural convection heat transfer in a differentially heated square enclosure with a heat generating-conducting circular cylinder at different diagonal locations, 6th International Advanced Technologies Symposium Proceedings (IATS'11), 16-18 May, Elazığ, Turkey, 2011, pp. 13–19.

[19] C. Butler, D. Newport, M. Geron, Natural convection experiments on a heated horizontal cylinder in a differentially heated square cavity, Experimental Thermal and Fluid Science 44 (2013) 199–208.

[20] H. Yüncü, S. Yamaç, Laminar natural convective heat transfer in an air-filled parallelogramic cavity, International Communications in Heat and Mass Transfer 18 (4) (1991) 559–568.

[21] V. Costa, Double-diffusive natural convection in parallelogrammic enclosures, International Journal of Heat and Mass Transfer 47 (2004) 2913–2926.

[22] A. Baïri, Transient free convection in passive buildings using 2D air-filled parallelogram-shaped enclosures with discrete isothermal heat sources, Energy and Buildings 43 (2010) 366–373.

[23] H. Saleh, S. Basriati, I. Hashim, Solutions of natural convection of nanofluids in a parallelogrammic enclosure by finite difference method, Jurnal Matematika and Sains 16 (2) (2011) 807–823.

[24] A. Baïri, Correlations for transient natural convection in parallelogrammic enclosures with isothermal hot wall, Applied Thermal Engineering 51 (2013) 833–838.

[25] A. Baïri, J. Garcia de Maria, Nu-Ra-Fo correlations for transient free convection in 2D convective diode cavities with discrete heat sources, International Journal of Heat and Mass Transfer 57 (2013) 623–628.

[26] K. Hoffmann, Computational Fluid Dynamics for Engineers, Engineering Education System Publications, Texas, U.S.A., 1989

[27] B. Kim, D. Lee, M. Ha, H. Yoon, A numerical study of natural convection in a square enclosure with a circular cylinder at different vertical locations, International Journal of Heat and Mass Transfer 51 (2008) 1888–1906.

[28] F. Moukalled, S. Acharya, Natural convection in the annulus between concentric horizontal circular and square cylinders, Journal of Thermophysics Heat Transfer 10 (1996) 524–531.